

# Prospects to measure neutrino oscillation pattern with very large area underground detector at very long baselines

V. Ammosov, V. Garkusha, A. Ivanilov, V. Kabachenko,  
E. Melnikov, F. Novoskoltsev, A. Soldatov, A. Zaitsev

*Institute for High Energy Physics,  
RU-142284 Protvino, Moscow region, Russia*

## Abstract

The concept of a very long baseline neutrino experiment with quasi monochromatic neutrino beam and very large area underground detector is discussed. The detector could be placed in the existing 20 km tunnel at IHEP, Protvino. The High Intensity Proton Accelerators (HIPA) which are planned to be built in Japan (JAERI-KEK, baseline of  $\sim 7000$  km) and Germany (GSI, baseline of  $\sim 2000$  km) as well as the Main Injector at Fermilab ( $\sim 7600$  km) are considered as possible sources of neutrino beams. The oscillations are analysed in the three-neutrino scheme taking into account terrestrial matter effects. In the proposed experiment it is feasible to observe the oscillation pattern as a unique proof of the existence of neutrino oscillations. Precise measurements of disappearance oscillation parameters of the muon neutrinos and antineutrinos can be done within a reasonable time.

# 1 Introduction

The observation of the atmospheric  $\nu_\mu$  disappearance [1, 2] stimulated an impressive number of proposals of new experiments with neutrino beams from proton synchrotrons [3, 4, 5, 6, 7, 8] and from neutrino factories [9]. Main goals of this new generation of experiments are the ultimate confirmation of neutrino oscillations and precise measurements of oscillation parameters.

Very long baseline (VLBL) neutrino-oscillation experiments with very large area (VLA) detectors are especially effective to observe the neutrino oscillation patterns and to measure precisely oscillation parameters. Here we consider the prospects to use underground detector placed in the existing UNK tunnel to carry out these measurements. As a source for neutrino beams we consider the high intensity proton accelerators which are planned to be built in Japan (JAERI-KEK, Tokaimura, baseline of  $\sim 7000$  km) and Germany (GSI, Darmstadt, baseline of  $\sim 2000$  km) as well as the existing Main Injector at Fermilab ( $\sim 7600$  km).

In the second section the physics justification of the proposed approach is given. The concept of a possible experimental lay-out including a neutrino focusing system and UNK underground detector are described in the third section. Physics performance is outlined in the fourth section. The last section is devoted to conclusion.

## 2 Physics motivation

We propose to measure the  $\nu_\mu$  and  $\bar{\nu}_\mu$  survival probabilities  $P(\nu_\mu(\bar{\nu}_\mu) \rightarrow \nu_\mu(\bar{\nu}_\mu))$  as a function of the neutrino energy. The UNK underground detector will register muons from  $\nu_\mu$  and  $\bar{\nu}_\mu$  charged current (CC) interactions in surrounding soil mainly. Expected effective mass will be at a  $\sim 1$  Mton level for a few GeV neutrino energy.

The motivation of the oscillation approach is based on the observation of atmospheric  $\nu_\mu$  disappearance and a small level, if any, of reactor  $\nu_e$  disappearance. Existing experimental data for the muon (electron) neutrino disappearance are analyzed in terms of the simple formula for oscillation probability  $P(\nu_\mu(\nu_e) \rightarrow \nu_\mu(\nu_e)) = 1 - I_{\mu(e)} \cdot \sin^2(1.27 \cdot \Delta m^2 \cdot L/E)$  between two neutrino of different flavours (see Table 1 for the experimental restrictions on the parameters).

**Table 1.** Summary of experimental results on neutrino disappearance.

Experiments	Best values	Allowed region
disappearance of atmospheric $\nu_\mu$ [10]	$I_\mu = 1.$ $\Delta m^2 = 2.5 \cdot 10^{-3} \text{ eV}^2$	$I_\mu > 0.84$ (99% CL) $1.2 \cdot 10^{-3} < \Delta m^2 < 4 \cdot 10^{-3} \text{ eV}^2$ (99% CL)
disappearance of reactor $\bar{\nu}_e$ [11]	–	$I_e < 0.1$ (90% CL)

At  $\Delta m^2 = 2.5 \cdot 10^{-3} \text{ eV}^2$  and with a few GeV neutrino energy the oscillation length is in the region of  $10^3 - 10^4$  km. Therefore, the measurement of the  $P(\nu_\mu(\bar{\nu}_\mu) \rightarrow \nu_\mu(\bar{\nu}_\mu))$  probability as a function of neutrino energy is a natural way to observe the neutrino oscillation pattern and to measure precisely the oscillation parameters for this pattern in the VLBL neutrino experiments.

The observation of atmospheric  $\nu_\mu$  disappearance is just an indication on neutrino oscillations but not a definite proof of it. Within the proposed approach different aspects of neutrino physics could be studied:

- Measurement of  $\nu_\mu$  and  $\bar{\nu}_\mu$  disappearance patterns.

In the case of a simple oscillation pattern  $P(\nu_\mu \rightarrow \nu_\mu) = 1 - I_\mu \cdot \sin^2(1.27 \cdot \Delta m^2 \cdot L/E)$  the precise measurements of  $\Delta m^2$  and  $I_\mu$  can be done for  $\nu_\mu$  and  $\bar{\nu}_\mu$ .

- Search for no oscillations or non-standard oscillations.

The models of neutrino disappearance by decay [12] or nonstandard oscillations due to flavour changing neutrino interactions [13] could be checked with high sensitivity. Observation of more complicated oscillation pattern could be a signal, for example, of large extra dimensions [14].

- Measurement of the difference  $\Delta_\mu = P(\nu_\mu \rightarrow \nu_\mu) - P(\bar{\nu}_\mu \rightarrow \bar{\nu}_\mu)$ .

It can come from a fake *CPT* violation due to the terrestrial matter effects [15] and can be from a genuine *CPT* violation if it exists [16]. As fake *CPT* violation depends on the *CP*-violating phase, the proposed experiment could provide information on it as well.

Below we consider the simple oscillation model in vacuum as the baseline, concentrating on the ability to observe the oscillation pattern.

Fig. 1 shows the  $\nu_\mu$  and  $\nu_e$  survival probabilities as functions of  $L/E$ . Arrows indicate the maximal  $L/E$  values which can be reached with the MINOS [5], the CERN-Gran Sasso (CNGS) [6], the JHF-SK [7] and the CERN Neutrino Factory (CNF) [9] planned experiments.

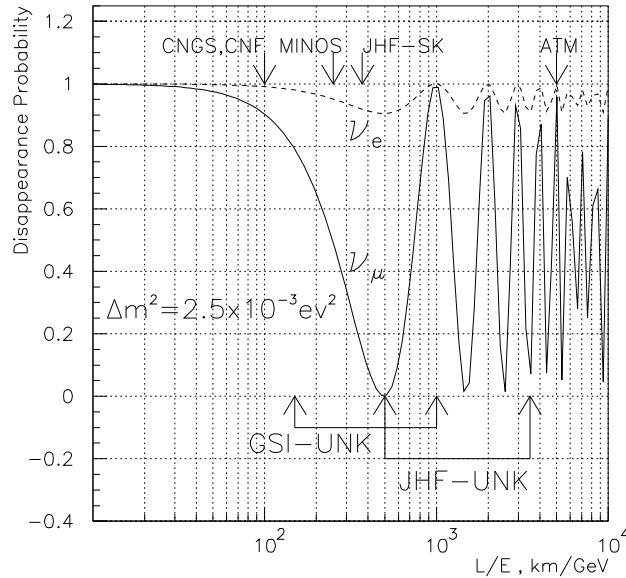


**Fig. 1.**  $P(\nu_\mu \rightarrow \nu_\mu)$  and  $P(\nu_e \rightarrow \nu_e)$  survival probabilities.

As it is seen in the figure CNF [9], CNGS [6] and MINOS [5] projects are at the beginning of the first wave of the oscillation curve, where oscillation patterns are not

seen. The JHF-SK project [7] has some chance to observe an oscillation pattern for  $\Delta m^2 > 3 \cdot 10^{-3} \text{ eV}^2$ .

As one can see in the figure the oscillation pattern in principle could be measured for the atmospheric  $\nu_\mu$ . However to do this, a precise reconstruction of the neutrino direction is needed to obtain the neutrino pass length. In the SK and MACRO detectors the neutrino direction is defined from the direction of muons which have wide angular distribution at low neutrino energy ( $\langle E_{\nu_\mu} \rangle = 2.4 \text{ GeV}$ ). Therefore, only the average disappearance was observed. Thus the oscillation curve is clearly visible if

- oscillation phase  $\phi_{osc} = 1.27 \cdot \Delta m^2 \cdot L/E \approx (2n + 1) \cdot \pi/2$ ,  $n = 0, 1, \dots$ ;
- error  $\delta\phi_{osc} < \pi/4$ .

Translation of these conditions to the energy resolution gives

$$\frac{\delta E_\nu}{E_\nu} < \frac{1}{2(2n + 1)}.$$

It means that the soft restriction is for  $n = 0$  and  $1$ , i.e., for the first and the second minima.

If we look at the Earth globes, the 1-st condition can be fulfilled if neutrino beams are sent to Protvino from the Fermilab MI, the JHF or the GSI (see expected JHF-UNK and GSI-UNK  $L/E$  regions on Fig. 1). In the Table 2 the possible characteristics of beams from the MI, the JHF and the GSI are presented.

**Table 2.** Comparison of neutrino sources for UNK VLBL neutrino oscillation experiment.

Parameter	JHF, Japan	GSI, Germany*	MI FNAL, USA
Baseline from the UNK, km	7000	2000	7600
Tilt angle, degree	33	9	34
Proton momentum, GeV/c	50	50	120
Cycle time, s	3	3	2
One turn time, $\mu\text{s}$	5	4	10
Proton intensity/spill	$3.3 \cdot 10^{14}$	$1 \cdot 10^{14}$	$4 \cdot 10^{13}$
Protons/s	$1 \cdot 10^{14}$	$3 \cdot 10^{13}$	$2 \cdot 10^{13}$
$\pi^+$ yield/p at 7 GeV/c	0.05	0.05	0.12
$\pi^+$ yield/s at 7 GeV/c	$5 \cdot 10^{12}$	$1.7 \cdot 10^{12}$	$2.4 \cdot 10^{12}$
duty factor	$1.7 \cdot 10^{-6}$	$1.3 \cdot 10^{-6}$	$5 \cdot 10^{-6}$

\* assumed parameters

Below we consider the JHF and the GSI as neutrino beam sites in comparison.

### 3 Experimental lay-out

#### 3.1 Concept of experiment

Sketch of the general experimental lay-out is shown in Fig. 2.

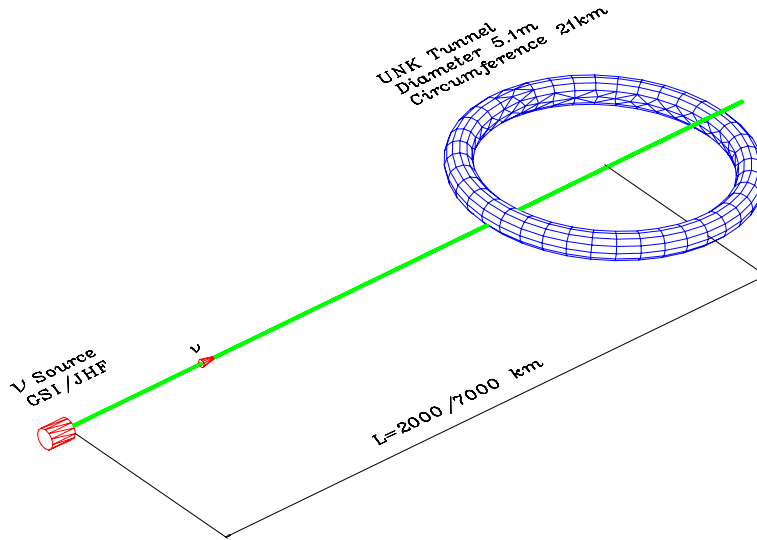


**Fig. 2.** General experimental lay-out.

Far neutrino source from the JHF (baseline of 7000 km) or GSI (baseline of 2000 km) have to point to the UNK tunnel which is  $\sim 50$  m underground in average. For such kind of distances, to have enough statistics, we should think about a detector with effective mass at the 1 Mton level. In such a case it is possible to use the surrounding soil of the UNK tunnel as neutrino target. It is proposed to cover the UNK tunnel walls by scintillation counters. For such an experimental concept, the UNK detector, which can be considered as a huge double scintillator counter, will count mainly muons from  $\nu_\mu$  ( $\bar{\nu}_\mu$ ) CC interactions in the surrounding soil.

The circumference length of the UNK tunnel is  $\sim 21$  km, and the diameter is  $\sim 5$  m. It means that an area of about  $\sim 10^5$  m<sup>2</sup> can be used for a very long baseline neutrino experiment. Dimensions and time resolution of individual scintillation counters will allow us to select muons from the expected neutrino direction.

To suppress the cosmic ray background the fast (one turn) extraction of the proton beam and the synchronization of a neutrino source and of the UNK detector [17] are ultimately needed.

To observe the neutrino oscillation pattern we intend to use a few (at least three) neutrino energy settings with a reasonable energy resolution and just count the double coincidences in the UNK detector. Ratios of the measured to expected counts at different energy settings will provide the possibility to observe  $\nu_\mu$  and  $\bar{\nu}_\mu$  oscillation patterns in the disappearance mode.

If we assume that at least the  $n = 1$  minimum should be detected then

$$\frac{\delta E_\nu}{E_\nu} < 0.15.$$

The ideal  $\nu_\mu$  disappearance curves and also the smeared curves for  $\delta E_\nu/E_\nu = 0.36$  (a WB like beam) and  $\delta E_\nu/E_\nu = 0.15$  (a NB like beam) as a function of the neutrino energy for

$\Delta m^2 = 2.5 \cdot 10^{-3} \text{ eV}^2$  for the GSI and JHF cases are shown in Fig. 3.

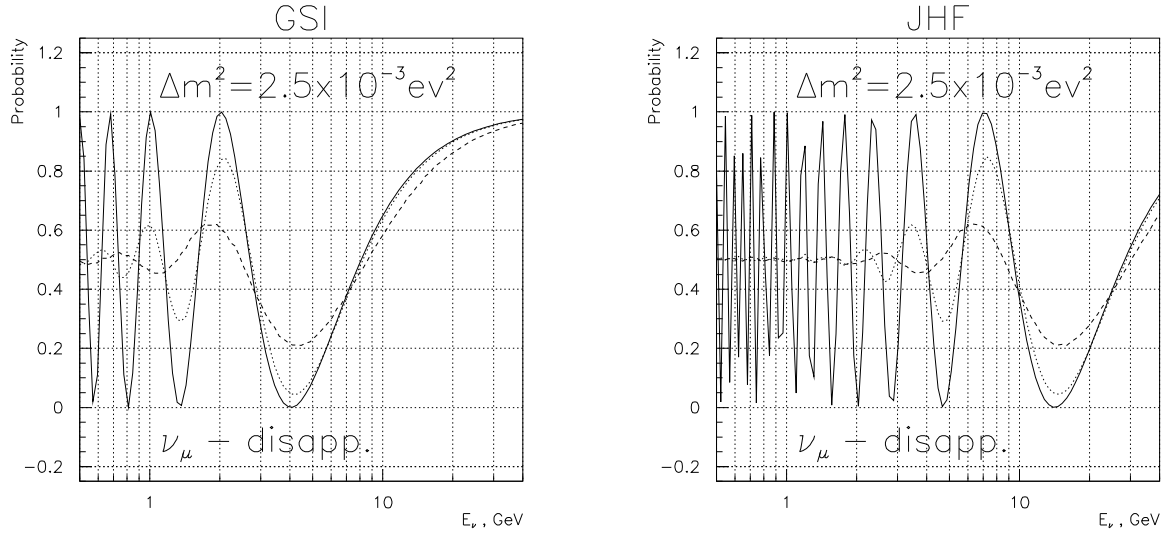


**Fig. 3.** Ideal (solid line), smeared for  $\delta E_\nu/E_\nu = 0.36$  (dashed line) and for  $\delta E_\nu/E_\nu = 0.15$  (dotted line) oscillation curves for the GSI and the JHF cases.

The importance of the  $\delta E_\nu/E_\nu = 0.15$  condition for a clear observation of the neutrino oscillation pattern is seen from this figure.

The proposed concept can be considered as a further development of the atmospheric neutrino experiments with upward-down-going muons. Here we already know:

- the exact distance from source to detector;
- the type of neutrino ( $\nu_\mu$  or  $\bar{\nu}_\mu$ );
- the neutrino energy.

### 3.2 Concept of the neutrino focusing system

To estimate the possible  $\nu_\mu$  and  $\bar{\nu}_\mu$  event rates in the UNK detector we used the focusing system based on the magnetic horns, which were optimized for the NuMI Project [18]. This focusing system (Fig. 4) can provide desired  $\delta E_\nu/E_\nu = 0.15$  condition.

The 50 GeV primary proton beam is used to produce pions in the  $\sim 2$  interaction lengths graphite target T. Two 3 m long magnetic horns H1–H2 with parabolic shaped inner conductors are used to focus the resulting pion beam down a drift space where pions will decay to muon neutrinos. Four 2 m long dipoles B1–B2 with 400 mm gaps are used to obtain a beam of secondaries with relatively small  $\Delta p/p$ . The total length of the decay region is equal to 400 m including the 40 m length target area and the 360 m length decay pipe of 1 m radius.

This focusing system may be tuned to different neutrino energy ranges by scaling the dipole currents and by corresponding adjustment of the target location, keeping the current in both horns at its nominal value of 200 kA. Energy spectra of  $\nu_\mu$  and  $\bar{\nu}_\mu$  CC events in the UNK detector are shown in Fig. 5 for a few different neutrino energy settings.

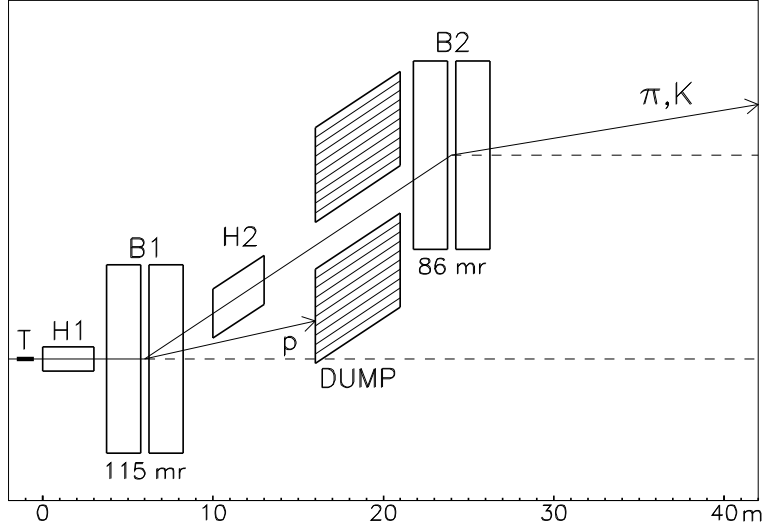


**Fig. 4.** The layout of the focusing system.

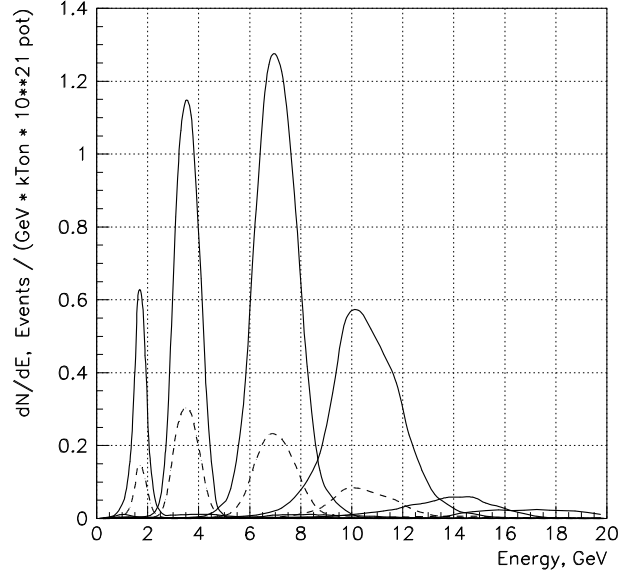


**Fig. 5.** Energy spectra of the  $\nu_\mu$  (solid lines) and  $\bar{\nu}_\mu$  (dashed lines) CC events in the UNK detector for the 1.7, 3.5, 7.0, 10.5 and 14.0 GeV energy settings.

**Table 3.** Focusing system and neutrino beam parameters. Target positions are given with respect to the upstream end of the first horn. The baseline is 7000 km.

Beam energy range, GeV	1.0–2.3	2.3–5.0	5.0–9.0	6.0–15.	8.0–19.
Target $Z_{upstream}$ , m	−0.34	−0.34	−1.94	−2.64	−3.34
Mean energy, GeV	1.7	3.5	7.0	10.5	14.0
Energy spread HWHH, %	~16	~16	~14	~14	~13
$\nu_\mu$ events/kTon/ $10^{21}$ pot	0.45	1.5	2.8	2.1	0.33
Fraction of $\bar{\nu}_\mu$ events, %	0.8	0.4	0.3	$\leq 0.3$	$\leq 0.3$
$\bar{\nu}_\mu$ events/kTon/ $10^{21}$ pot	0.11	0.38	0.49	0.27	0.033
Fraction of $\nu_\mu$ events, %	$\leq 16$	$\leq 6$	$\leq 10$	$\leq 17$	$\leq 30$

The optics layout, event rates and backgrounds are summarized in Table 3.

One should note the following:

1. Three tune-ups of the considered focusing system span together the energy range from 1.7 to 7 GeV and tune-ups intermediate between these three can be easily achieved. The more complicated configuration of a focusing system (with obviously smaller focusing efficiency for some particular tune-up) is required to provide neutrino beams with  $\langle E_\nu \rangle$  from 1.7 up to 13–14 GeV.
2. To obtain more intensive neutrino beams with  $\sim 3$  and 6 events/kTon/ $10^{21}$  pot for  $\langle E_\nu \rangle = 3.5$  and 7.0 GeV, respectively, one may use a rectilinear focusing system with horns at the same positions but without dipoles. In this case the energy spreads of beams (HWHH) are of about 37%.

### 3.3 Concept of detector

The proposed baseline design for the UNK detector relies on the known plastic scintillator extrusion technology. The UNK detector uses extruded plastic scintillator which is read out by wavelength-shifting (WLS) bars coupled to photomultipliers. Some of the features which make plastic scintillator attractive are:

- High efficiency for crossing particles registration;
- Fast scintillation timing;
- Ease of calibration procedure;
- Long-term stability and reliability;
- Production potential - the plastic scintillator facility at IHEP, Protvino allows to produce the full amount of scintillator within 2–3 years;
- Low maintenance — the plastic scintillator detector is quite robust and will require little maintenance in the underground tunnel conditions.

The proposed detector consists of scintillating counters (10 mm thickness, 50 cm width and up to 6 m length) which cover the walls of the UNK tunnel. The proposed transverse coverage of the UNK tunnel is presented in Fig. 6.

The adjacent scintillation counters are coupled with each other through the WLS-shifter (3 mm thickness, 10 mm width) for light collection along the 6 m length (see Fig. 7) and thus all counters in one 6 m cylindrical section form the continuous circular chain.

Scintillation counters based on polystyrene with PTP and POPOP fluorescence dopants can be produced by extrusion technology at the IHEP, Protvino scintillator production facility. The PMMA-based WLS-shifter bars with Kumarin-30 Fluorescence doping will be used. The light attenuation length for such WLS-shifter is of 3 m [19, 20]. The scintillator (decay time 2.3 ns; emission peak 420 nm; attenuation length 20 cm at 420 nm) and WLS bars (decay time 2.7 ns; emission peak 460 nm; attenuation length up to 3 m at 460 nm) are wrapped in white material (e.g. TYVEK) and black paper.



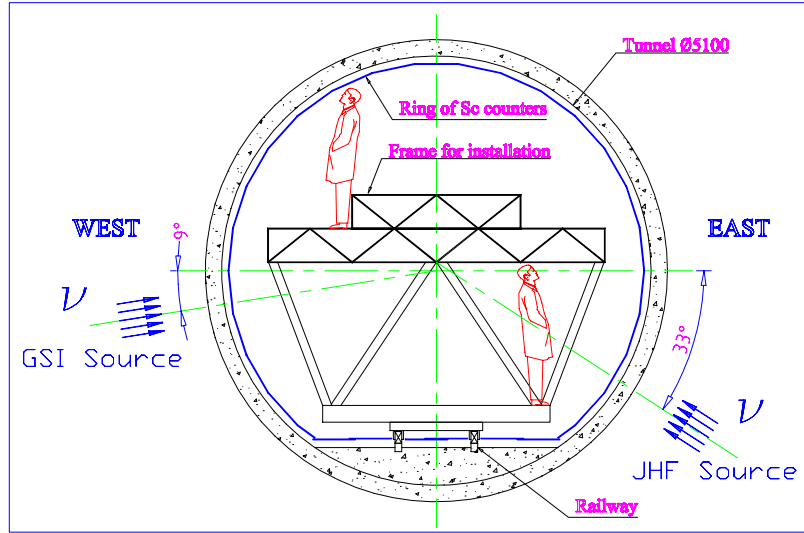


**Fig. 6.** The proposed transverse coverage of the UNK tunnel.

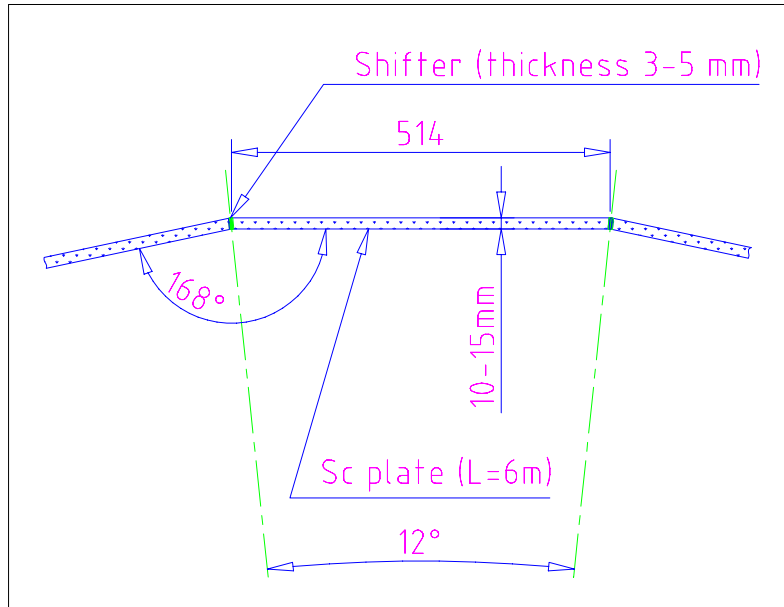


**Fig. 7.** The scintillation counters coupling.

The light is collected from both sides of the WLS-shifter bar using the 1" PMTs. A green extended phototube FEU-115M from MELZ (Moscow, Russia) [21] can be used for light collection. The PMT has an average quantum efficiency of 15% at 500 nm with a gain around  $10^6$ . The estimations show that the signal for muon, crossing the scintillating strip near the PMT will be  $\sim 25$  ph.el. Signals from phototubes are delivered to the QDCs and TDCs.

The coordinate resolution is estimated as  $\sim 30$  cm along the tile and  $\sim 10$  cm in transversal direction using the TDC and QDC information.

Each cylinder section with diameter 5.1 m and length 6 m, contains 32 counters. Trigger is defined as coincidence of at least two nonadjacent scintillation counters and performed only within neutrino source spill time.

In the Table 4 main features of the UNK underground detector are given.

**Table 4.** Main parameters of the UNK detector.

Item	Value
counter dimensions	$10 \times 500 \times 6000 \text{ mm}^3$
time resolution	1 ns
coordinate resolution	25 cm
inefficiency	$4 \cdot 10^{-5}$
number of counters in the cylinder section	32
total number of sections	3500
total number of counters	112000
total weight of scintillator	3400 Ton
total volume of the UNK tunnel	$400000 \text{ m}^3$

## 4 Physics performance

### 4.1 Statistics

To estimate the statistics of the experiment we performed a Monte-Carlo simulation of the detector response for the simple oscillation approach of vacuum oscillations  $P(\nu_\mu \rightarrow \nu_\mu) = 1 - I_\mu \cdot \sin^2(1.27 \cdot \Delta m^2 \cdot L/E)$ . We used the coverage of the UNK tunnel shown in Fig. 6. We concentrated our study on the selection of  $\nu_\mu$  and  $\bar{\nu}_\mu$  CC events. The following criteria were applied for selection:

1. Presence of two hits in two non-adjacent scintillation counters.
2. Time difference between hits greater than 10 ns.
3. “Tracks” pointing to the neutrino source.
4. Angle between neutrino and “track” directions less than  $30^\circ$  in each plane, and “track” direction below horizon.
5.  $0.7 < \beta = v/c < 1$ .

In the Table 5 the CC and NC event rates for different neutrino energy settings are presented.

**Table 5.** Number of events in case of no oscillation for  $10^7$  s running time for each energy setting.

$E_\nu$ , GeV	$\nu_\mu$				$\bar{\nu}_\mu$			
	CC		NC		CC		NC	
	GSI	JHF	GSI	JHF	GSI	JHF	GSI	JHF
1.7	560	160	12	4	150	50	3	0.7
3.5	3400	1100	70	18	1100	360	15	3.3
7.0	12000	4200	200	40	2800	1000	30	9
14.0	2800	1000	34	9	380	130	4	1.1

As it is seen a reasonable number of CC events can be selected for the NBB with  $E_\nu > 2$  GeV within one year of running ( $10^7$  s) for the JHF and GSI cases.

Fig. 8 shows the dependence of the detector effective mass for the CC and NC events as a function of the neutrino energy. Fig. 9 shows (a) CC  $\bar{\nu}_\mu/\nu_\mu$  effective mass ratio and (b)  $\nu_\mu\text{NC}/\nu_\mu\text{CC}$  and  $\bar{\nu}_\mu\text{NC}/\bar{\nu}_\mu\text{CC}$  event ratios.

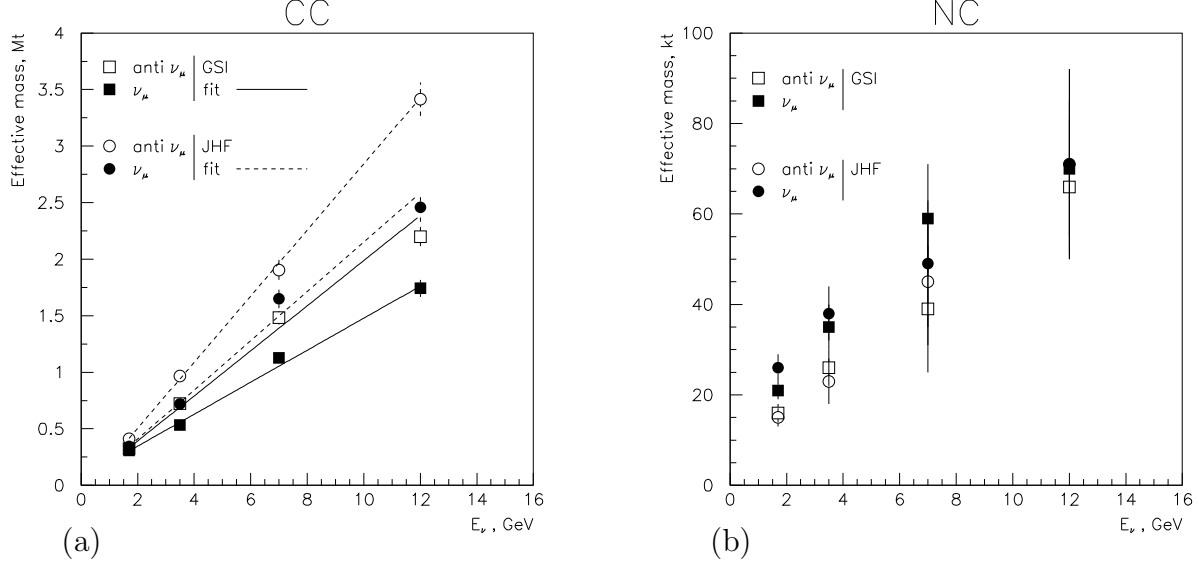


**Fig. 8.** Effective mass for (a) CC  $\nu_\mu$  and  $\bar{\nu}_\mu$  events, (b) NC  $\nu_\mu$  and  $\bar{\nu}_\mu$  events as a function of the neutrino energy.

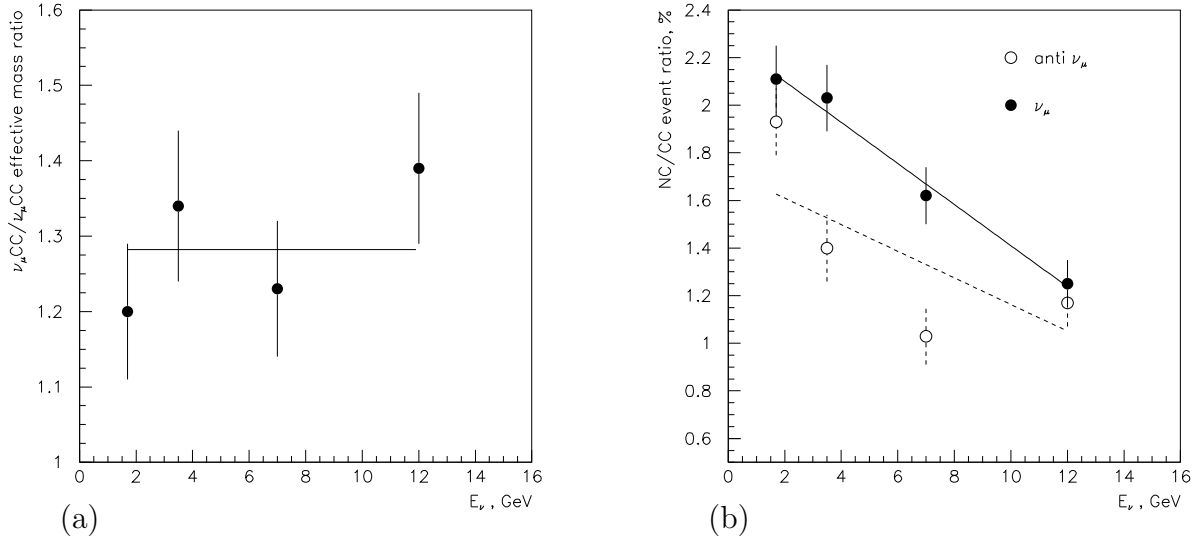


**Fig. 9.** Ratio (a)  $\bar{\nu}_\mu\text{CC}/\nu_\mu\text{CC}$  for effective masses, (b)  $\nu_\mu\text{NC}/\nu_\mu\text{CC}$  and  $\bar{\nu}_\mu\text{NC}/\bar{\nu}_\mu\text{CC}$  for events.

As it is seen the CC effective mass linearly increases with the increase of  $E_\nu$  reflecting the muon range increase. Slight increase of the NC effective mass is seen as well. The  $\bar{\nu}_\mu\text{CC}/\nu_\mu\text{CC}$  ratio for effective masses is  $\sim 1.3$  due to the different  $y$ -dependence of  $\bar{\nu}_\mu\text{CC}$  and  $\nu_\mu\text{CC}$  cross sections. The NC/CC ratio is about few percent for  $E_\nu \sim 2$  GeV. The

**Table 6.** Estimation of running time needed for  $10^3$  events at each energy setting.

$\nu$ source	$E_\nu$ , GeV	$\nu_\mu$			$\bar{\nu}_\mu$		
		Nev	pot, $\cdot 10^{21}$	time, $\cdot 10^7$ s	Nev	pot, $\cdot 10^{21}$	time, $\cdot 10^7$ s
JHF	5.7	1000	0.35	0.35	1000	1.4	1.4
	7.1	1000	0.23	0.23	1000	1.1	1.1
	9.4	1000	0.32	0.32	1000	1.3	1.3
	14.0	1000	1.00	1.00	-	-	-
		Total	1.9	1.9	Total	3.8	3.8
GSI	2.0	1000	0.35	1.04	400	0.56	1.67
	4.0	1000	0.07	0.22	1000	0.24	0.72
	8.0	1000	0.02	0.07	1000	0.12	0.36
		Total	0.44	1.33	Total	0.92	2.75

efficiency for  $\nu_e$ CC and  $\nu_\tau$ CC is comparable with that for  $\nu_\mu$ NC. Thus such kind of detector is a natural  $\nu_\mu$ CC event selector.

To estimate the experimental sensitivity of the oscillation pattern measurements we select three-four neutrino energy settings where oscillations are maximal or minimal for  $\Delta m^2 = 2.5 \cdot 10^{-3} \text{ eV}^2$ . The statistics for each setting was restricted to 1000 CC events assuming that there is no oscillation. This restriction is reasonable assuming systematic uncertainties of about  $\sim 3\%$  for the expected number of events using the proposed NBB. In the Table 6 we present these energy settings with the expected statistics (no oscillation), values of pot's and exposure times for  $\nu_\mu$  and  $\bar{\nu}_\mu$  cases for the JHF and the GSI. As it is seen from this table the oscillation pattern measurements can be carried out in a reasonable time even in the worse  $\bar{\nu}_\mu$  case.

## 4.2 Background

The experiment sensitivity depends on the background level. It is expected that the main background is due to the cosmic muons. Three sources of this background can be considered:

- $\mu b1$  cosmic muons which coincide in direction with accepted solid angle of muons from the neutrino source;
- $\mu b2$  cosmic muons which interact in the surrounding soil and produce through-going secondary particles within the accepted neutrino source direction;
- $\mu b3$  cosmic muons which move in the direction opposite to the accepted solid angle for the neutrino source but with wrong TOF identification.

The  $\mu b1$  background can be estimated knowing the muon flux as a function of the zenith angle  $\theta$ . Fig. 10 shows this muon flux for the UNK detector for an average depth of 50 m. It is seen that the flux sharply drops down to the value of  $4 \cdot 10^{-7} \mu \cdot \text{m}^{-2} \cdot \text{sr}^{-1} \cdot \text{s}^{-1}$  at  $\theta = 90^\circ$ . This constant value for  $\theta > 89.5^\circ$  is defined by muons from atmospheric neutrino interactions. It means that we should accept only muons below horizon ( $\theta > 90^\circ$ ). This cut

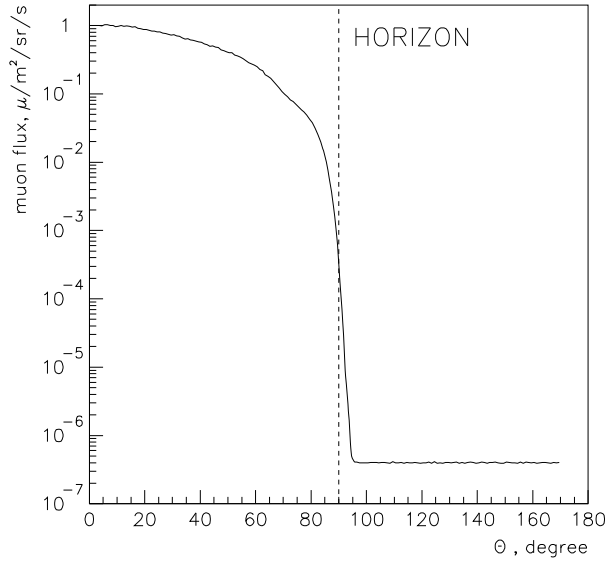


**Fig. 10.** Muon flux as a function of zenith angle  $\theta$  for the UNK underground detector (50 m depth in average).

reduces the statistics for the GSI neutrino source by  $\sim 20\%$ . We estimate this background as  $N_{\mu b1} = T \cdot \Phi(\mu) \cdot \Omega \cdot S \cdot D = 0.8 \mu$  for an exposure time  $T = 10^7$  s (one year), a solid angle  $\Omega = 1$  sr, a muon flux  $\Phi(\mu) = 4 \cdot 10^{-7} \mu \cdot \text{m}^{-2} \cdot \text{sr}^{-1} \cdot \text{s}^{-1}$ , a detector area  $S = 10^5$  m<sup>2</sup> and a duty factor  $D = 2 \cdot 10^{-6}$ .

The  $\mu b2$  background is estimated using the MACRO background measurements [22]. It was found that each down-going muon produces the  $2 \cdot 10^{-5}$  registered up-going particles. It is estimated that for the UNK detector this background is  $N_{\mu b2} = 40 \mu$  for one year exposure ( $T = 10^7$  s). Therefore, it is the most significant source of cosmic muon background. It can be further reduced using the RF structure of the beam.

We estimate the  $\mu b3$  background as the value of  $N_{\mu b3} = 0.2 \mu$  for  $10^7$ s assuming  $\Phi(\mu) = 1 \mu \cdot \text{m}^{-2} \cdot \text{sr}^{-1} \cdot \text{s}^{-1}$  and the  $6\sigma$  separation for the TOF system ( $10^{-7}$  probability for the Gaussian).

For the first glance the cosmic muon background is not so severe for our experimental conditions and is  $< 20\%$  for the worse  $\bar{\nu}_\mu$  case at low energies. However, it should be noted that the background is sensitive to the detector characteristics like tails of coordinate and time resolutions which were not taken into account. Obviously, a direct measurement of the background in the UNK tunnel is needed.

### 4.3 Sensitivity

To estimate the sensitivity of the UNK neutrino experiment to  $\nu_\mu$  disappearance oscillation parameters we used the values of  $\Delta m^2 = 2.5 \cdot 10^{-3}$  eV<sup>2</sup> and  $I_\mu = 0.95$  and selected the neutrino energy settings with the expected numbers of CC events (no oscillation) presented in Table 6. Fig. 11 shows the simulated probability values  $P = N_{osc}/N_{exp}$  with error bars, the fitted curve and the obtained ideal oscillation curve for the GSI and the JHF cases as examples for the identification and measurement of the neutrino oscillation patterns.

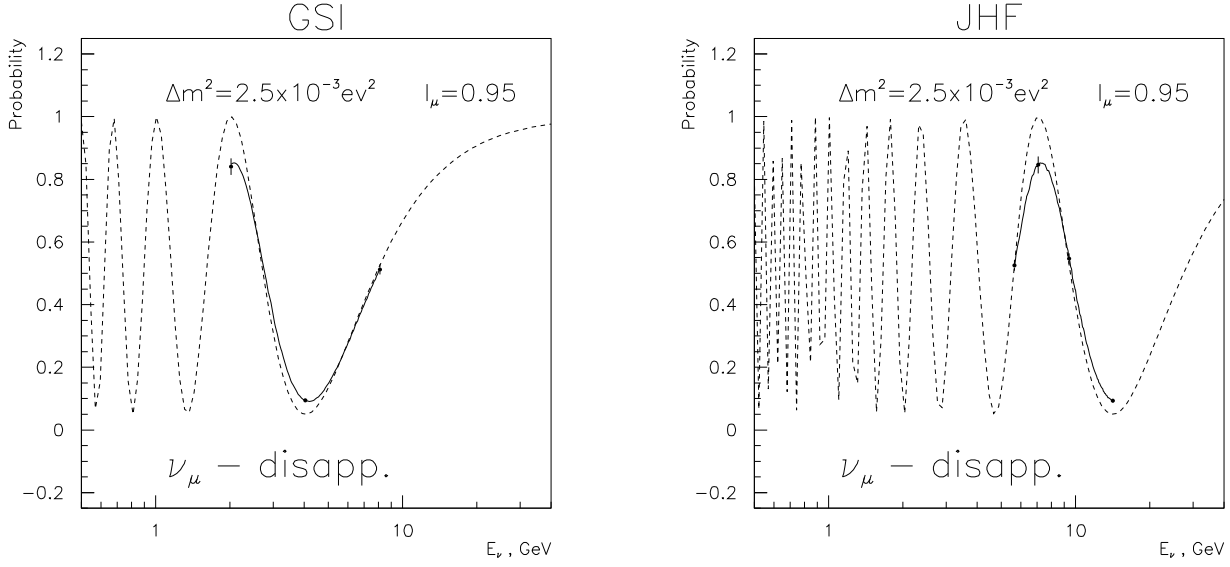


**Fig. 11.** Simulated oscillation pattern (full points), fitted (solid line) and ideal (dashed line) oscillation curves for the GSI and the JHF cases using of  $\nu_\mu$  data, presented in Table 6.

The estimated sensitivity for the GSI case is

$$\begin{aligned}\sigma_{\Delta m^2} &= 2.7 \cdot 10^{-5} \text{ eV}^2 \text{ and} \\ \sigma_{I_\mu} &= 0.01,\end{aligned}$$

and for the JHF case is

$$\begin{aligned}\sigma_{\Delta m^2} &= 1.5 \cdot 10^{-5} \text{ eV}^2 \text{ and} \\ \sigma_{I_\mu} &= 0.01.\end{aligned}$$

So, in this experiment the relative errors  $\sim 1\%$  can be achieved for  $\Delta m^2$  and  $I_\mu$ .

These sensitivities can be reached in the  $\Delta m^2$  regions as presented in Table 7.

**Table 7.** The  $\Delta m^2$  region accessible to the experiment.

$\nu$ source	$\Delta m^2$ in $10^{-3} \text{ eV}^2$
GSI	$1.5 < \Delta m^2 < 6$
JHF	$0.5 < \Delta m^2 < 4$

The measurement of  $\Delta_\mu = P(\nu_\mu \rightarrow \nu_\mu) - P(\bar{\nu}_\mu \rightarrow \bar{\nu}_\mu)$  as a function of the neutrino energy can allow to estimate the values of effective  $CPT$  violation parameters  $\delta_\mu = \Delta m^2 - \Delta \bar{m}^2$  and  $\epsilon_\mu = I_\mu - I_{\bar{\mu}}$  with a relative precision of  $\sim 2\%$  and of  $\sim 1\%$ , respectively.

Such a precision allows to observe oscillation or decay neutrino patterns, to measure precisely the neutrino oscillation parameters in the simple case of oscillation, to search for fake and genuine  $CPT$  violation effects at a few percent level and to search for complicated oscillation behaviour.

## 4.4 Terrestrial matter effects

The analysis given before was based on a simple approximate formula  $P(\nu_\mu \rightarrow \nu_\mu) = 1 - I_\mu \sin^2(1.27\Delta m^2 \cdot L/E)$  for two-neutrino oscillation in vacuum, which contain two independent parameters only. In this section we consider more realistic approach including terrestrial matter effects. We restrict ourselves only by analysis in the framework of mixing between three known neutrino. This scheme is compatible with the existing data on solar and atmospheric neutrino observation as well as reactor neutrino experiments. Four-neutrino scheme with light sterile neutrino is required only by LSND experiment, which is still not confirmed. Moreover, recent analysis tells us that this scheme is unsatisfactory as explanation of all experimental evidences for neutrino oscillations and is marginally acceptable [23].

In the case of three-neutrino scheme, unitary matrix which transforms neutrino mass eigenstates into flavour ones can be written in the standard form

$$U = \begin{pmatrix} c_{12}c_{13} & s_{12}c_{13} & \tilde{s}_{13}^* \\ -s_{12}c_{23} - c_{12}\tilde{s}_{13}s_{23} & c_{12}c_{23} - s_{12}\tilde{s}_{13}s_{23} & c_{13}s_{23} \\ s_{12}s_{23} - c_{12}\tilde{s}_{13}c_{23} & -c_{12}s_{23} - s_{12}\tilde{s}_{13}c_{23} & c_{13}c_{23} \end{pmatrix}, \quad (1)$$

where  $\tilde{s}_{13} = s_{13}e^{i\delta}$ ,  $s_{ij} \equiv \sin\theta_{ij}$  and  $c_{ij} \equiv \cos\theta_{ij}$ . The matrix has four independent parameters: three mixing angles  $\theta_{ij}$  ( $i < j$ ) and  $CP$  violating phase  $\delta$ . In general there exist two additional Majorana specific phases, but they do not contribute to the lepton number conserving oscillations and are omitted in Eq. 1. Four parameters in matrix  $U$ , together with two squared mass differences for neutrino, say  $\Delta m_{21}^2 \equiv m_2^2 - m_1^2$  and  $\Delta m_{32}^2 \equiv m_3^2 - m_2^2$ , form six parameter set which defines full oscillation pattern. At present, the best fit values for these parameters lie in two distinct statistically significant regions called *large mixing angle* (LMA) and *low mass* (LOW) [23]. They are the two solutions which we will keep in mind in further investigation. We do not intend to explore the all allowed parameter space. Rather, we are going to answer general questions such as the principal possibility to measure  $CP$  violation parameter  $\delta$  or the possibility to distinguish LMA and LOW solutions.

Differential equations which describe propagation of neutrino flavour states on a distance  $L$  look as follows

$$i\frac{d}{dL} \begin{pmatrix} \nu_e \\ \nu_\mu \\ \nu_\tau \end{pmatrix} = \left[ \frac{1}{2E} U \begin{pmatrix} -\Delta m_{21}^2 & 0 & 0 \\ 0 & 0 & 0 \\ 0 & 0 & \Delta m_{32}^2 \end{pmatrix} U^\dagger + \begin{pmatrix} A(L) & 0 & 0 \\ 0 & 0 & 0 \\ 0 & 0 & 0 \end{pmatrix} \right] \begin{pmatrix} \nu_e \\ \nu_\mu \\ \nu_\tau \end{pmatrix}, \quad (2)$$

$$A(L) = \frac{1}{\sqrt{2}} G_F N_A \rho(L).$$

Here  $E$  is the energy of neutrino beam,  $A(L)$  is the potential induced by coherent interaction of electron neutrinos with electrons in the matter,  $G_F$  is the Fermi constant,  $N_A$  is Avogadro's number and  $\rho(L)$  denotes the Earth matter density. Equations for antineutrinos are obtained from Eq. 2 by replacement  $(U, A) \rightarrow (U^*, -A)$ . Fake  $CPT$  violation appears due to the different sign at  $A$  for neutrino and antineutrino. In the vacuum  $P(\nu_\mu \rightarrow \nu_\mu) = P(\bar{\nu}_\mu \rightarrow \bar{\nu}_\mu)$ .

In our analysis we solve these equations numerically with density profile  $\rho(L)$  taken from the Preliminary Reference Earth Model [24]. As for the mixing angles and neutrino

squared mass differences, we choose two sets of the parameters corresponding to the aforementioned LMA and LOW regions

$$\begin{aligned}
& \Delta m_{21}^2 = 1.4 \cdot 10^{-4} \text{ eV}^2 \\
& \theta_{12} = 35^\circ \quad \text{Point 1 (LMA)} \\
& |\Delta m_{32}^2| = 2.5 \cdot 10^{-3} \text{ eV}^2 \\
& \theta_{23} = 40^\circ \\
& \theta_{13} = 13^\circ \\
& \Delta m_{21}^2 = 1.0 \cdot 10^{-7} \text{ eV}^2 \quad \text{Point 2 (LOW)} \\
& \theta_{12} = 35^\circ.
\end{aligned} \tag{3}$$

These values will be used as reference points in parameter space but we will also consider variations in some of parameters in the experimentally allowed limits.

To characterize the effects of fake  $CPT$  violation due to the non-zero matter density it is convenient to introduce asymmetry between  $\nu_\mu - \bar{\nu}_\mu$  oscillation probabilities

$$A_{CPT} = \frac{P(\nu_\mu \rightarrow \nu_\mu) - P(\bar{\nu}_\mu \rightarrow \bar{\nu}_\mu)}{P(\nu_\mu \rightarrow \nu_\mu) + P(\bar{\nu}_\mu \rightarrow \bar{\nu}_\mu)}. \tag{4}$$

Before discussion the results of our calculations we make some general remarks.

1. Without loss of generality one may take for mixing angles and phase in matrix  $U$  the following values

$$\theta_{ij} \in [0, \frac{\pi}{2}] \quad \text{and} \quad \delta \in [-\pi, \pi].$$

From Eq. 2 one can show that, in the constant matter density approximation,  $P(\nu_\mu(\bar{\nu}_\mu) \rightarrow \nu_\mu(\bar{\nu}_\mu))$  does not alter under the change  $\delta \rightarrow -\delta$ . The experiment under discussion could not distinguish  $\delta$  and  $-\delta$ .

2. When any of the mixing angles in matrix  $U$  is zero, the dependence on phase  $\delta$  in oscillation probabilities disappear. In the experimentally allowed parameter space  $\theta_{13}$  is the smallest angle and it is the only one which is compatible with zero ( $0 \leq s_{13}^2 \leq 0.05$  and zero value minimizes the  $\chi^2$  function for global fit of present data [23]).

3. In the limit  $\Delta m_{21}^2 \rightarrow 0$  the dependence on angle  $\theta_{12}$  and phase  $\delta$  is dropped out in Eq. 2. Therefore, there is no chance to determine these two parameters in discussed experiments when LOW solution is realized in Nature.

4. In the limit  $\Delta m_{21}^2 \rightarrow 0$ , the changing in sign of  $\Delta m_{32}^2$  is equivalent to passing from Eq. 2 for neutrinos to equations for antineutrinos, i.e.,  $P(\nu_\mu \rightarrow \nu_\mu; \Delta m_{32}^2) = P(\bar{\nu}_\mu \rightarrow \bar{\nu}_\mu; -\Delta m_{32}^2)$ . Therefore, the sign of asymmetry  $A_{CPT}$ , if not zero, may reflect the sign of  $\Delta m_{32}^2$  even in the case  $\Delta m_{21}^2 \neq 0$ .

5. For the LOW solution (for which  $\Delta m_{21}^2 = 0$  is very good approximation) the matter influence on oscillation pattern is sensitive to the value of  $\theta_{13}$ . At  $\theta_{13} = 0$  Eq. 2 decouples into two pieces: electron neutrino does not take part in oscillations while muon and tau neutrinos oscillate as in vacuum and  $A_{CPT}$  vanishes. This is not so for the LMA solution, zero value of  $\theta_{13}$  does not lead to the decoupling due to the non-negligible value of  $\Delta m_{21}^2$  and deviation of  $A_{CPT}$  from zero may be significant. Hence, the measurement of near zero value of  $A_{CPT}$  at all energies will point out on the LOW solution with small  $\theta_{13}$ .



**Numerical results** In all figures presented below we use the oscillation probability smeared with energy, assuming NB like beam with energy spread  $\delta E/E = 0.15$ .

Figs. 12 and 13 illustrate the matter influence on the oscillation profile for the case of GSI and JHF, respectively. All curves correspond to phase  $\delta = 0^\circ$  and  $\Delta m_{32}^2 > 0$ . The difference between neutrino and antineutrino oscillation curves is seen directly, especially it is impressive for the case of JHF. It is interesting to note, that in the last case there is not only difference in amplitude but also a phase shift, which reaches up to  $\sim 1$  GeV.

Asymmetry  $A_{CPT}$  is plotted in the Figs. 14 and 15 as function of beam peak energy. One can see that asymmetry has absolute maximum both for GSI and JHF cases. As for the JHF case, maximum in asymmetry appears near the position of the first maximum of the oscillation curve where the difference between neutrino and antineutrino probabilities is enormous. In the GSI case the absolute differences between neutrino and antineutrino at first minimum and maximum of oscillation curve are approximately the same and, therefore, maximum in asymmetry occurs at first oscillation minimum.

Thick lines in Figs. 14 and 15 corresponds to positive  $\Delta m_{32}^2$ , while thin lines to negative one. Solid lines in Figs. 14(b) and 15(b), which are for values of parameters at Point 2 (Eq. 3), demonstrate the reflection of asymmetry under the changing in sign of  $\Delta m_{32}^2$ . Such a behaviour is kept, in the energy region near the asymmetry maximum, even for the parameters at Point 1, in spite of the not so large hierarchy between  $\Delta m_{21}^2$  and  $\Delta m_{32}^2$ . Clear distinction between the positive and negative signs of  $\Delta m_{32}^2$  is lost only at lower energies. One may conclude that at energies near the asymmetry maximum the sign of  $\Delta m_{32}^2$  is defined unambiguously, whatever solution, LMA or LOW, is realized in Nature.

To illustrate the sensitivity to the angle  $\theta_{13}$  for LOW region we present in Figs. 14(b) and 15(b) the additional curves for asymmetry corresponded to  $s_{13}^2 = 0.01$  and  $0.03$ . It is clear that the JHF, in contrast to the GSI case, is in a position to resolve small values of angle  $\theta_{13}$ .

As was mentioned early, the experiment may be sensitive to the  $CP$  violating phase  $\delta$  only for LMA solution. In Figs. 14(a) and 15(a) solid lines present the asymmetry for  $\delta = 0$ , while dashed lines are for  $\delta = 180^\circ$ . One can see that at low energies, say, at  $\sim 1$  GeV, the values of asymmetry are large enough and clearly separated for these boundary values of  $\delta$ . It is in contrast with the behaviour of asymmetry for LOW region of parameters, where it approaches to zero at low energies. As a consequence, the observation of non-zero value of asymmetry at low energy will discriminate between LMA and LOW solutions, on the one hand, and will allow to determine the value of  $\delta$ , on the other hand. The measurement of near zero value of  $A_{CPT}$  at low energies will be less informative: there exist some values of parameters when oscillation patterns for LOW and LMA solutions are very close. Fig. 16 illustrates possible worse case to study for the parameters of Point 1 with  $\delta = 90^\circ$  and Point 2.

One should note that the using of NB like beam is important, first of all, for the precise measurement of the shape of oscillation curve and, hence, for the precise measurement of oscillation parameters like  $\Delta m^2$  or amplitude  $I_\mu$ . In contrast with this, the low energy measurement does not require NBB. Rather, one should use WB like beam to compensate the decreasing in statistics at low energies.

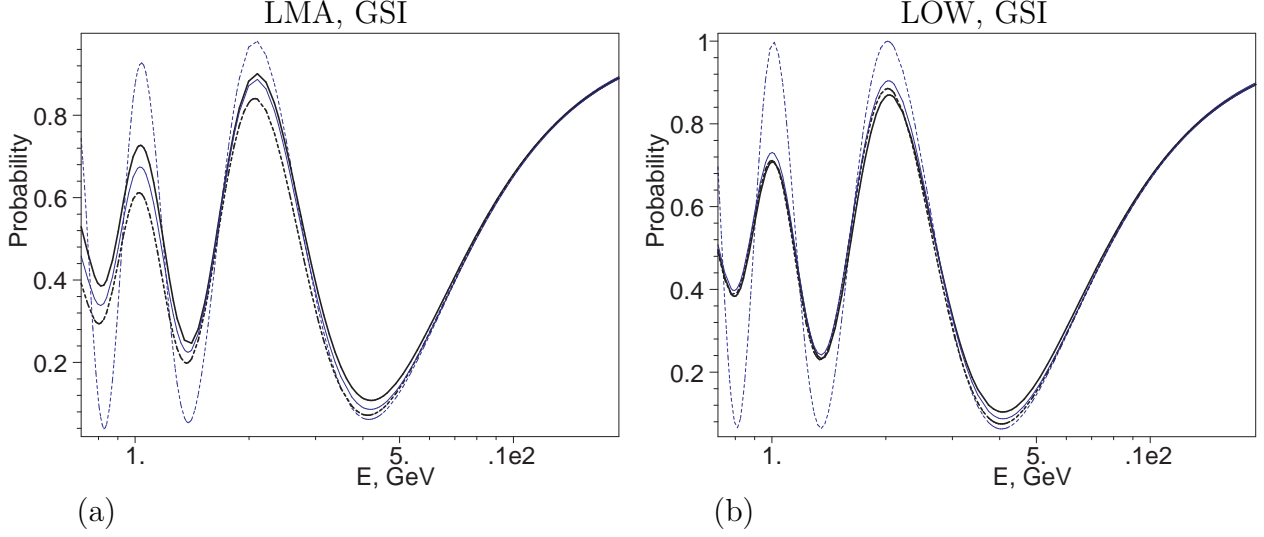


**Fig. 12.** Survival probability as function of beam energy for the GSI ( $L = 2000$  km): (a) Point 1, (b) Point 2 (Eq. 3). Thick solid line shows  $P(\nu_\mu \rightarrow \nu_\mu)$  in matter smeared with  $\delta E_\nu/E_\nu = 0.15$ , thick dashed line shows smeared  $P(\bar{\nu}_\mu \rightarrow \bar{\nu}_\mu)$  in matter. For comparison, smeared vacuum oscillation curve (thin solid line) and vacuum oscillation curve without smearing (thin dashed line) are also plotted. All curves correspond to  $\delta = 0^\circ$ .

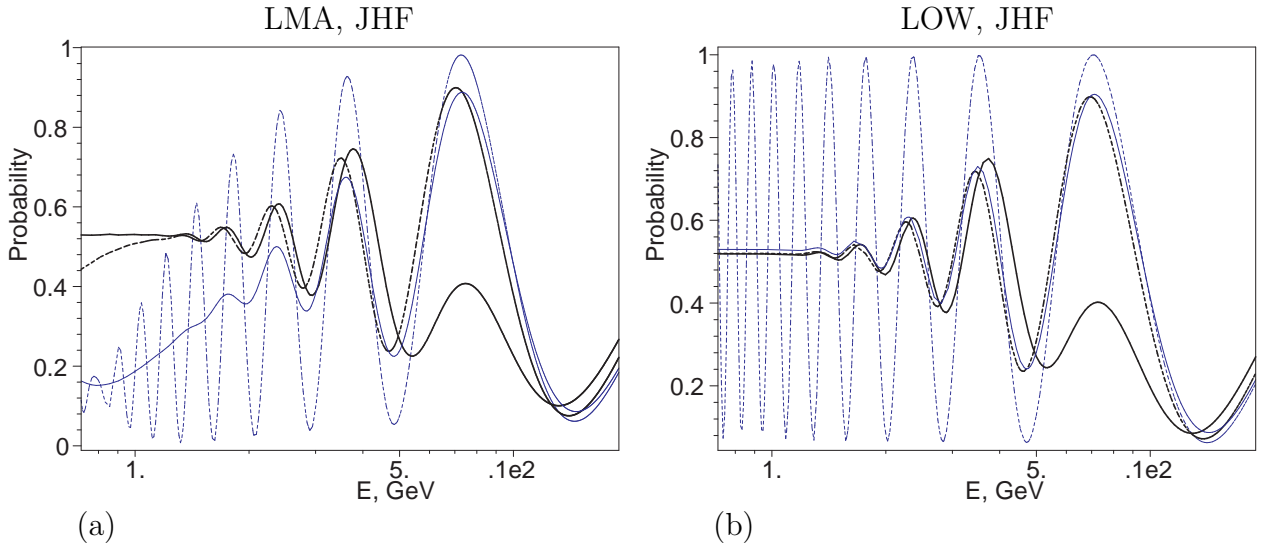


**Fig. 13.** The same as in Fig. 12, but for the JHF case ( $L = 7000$  km).

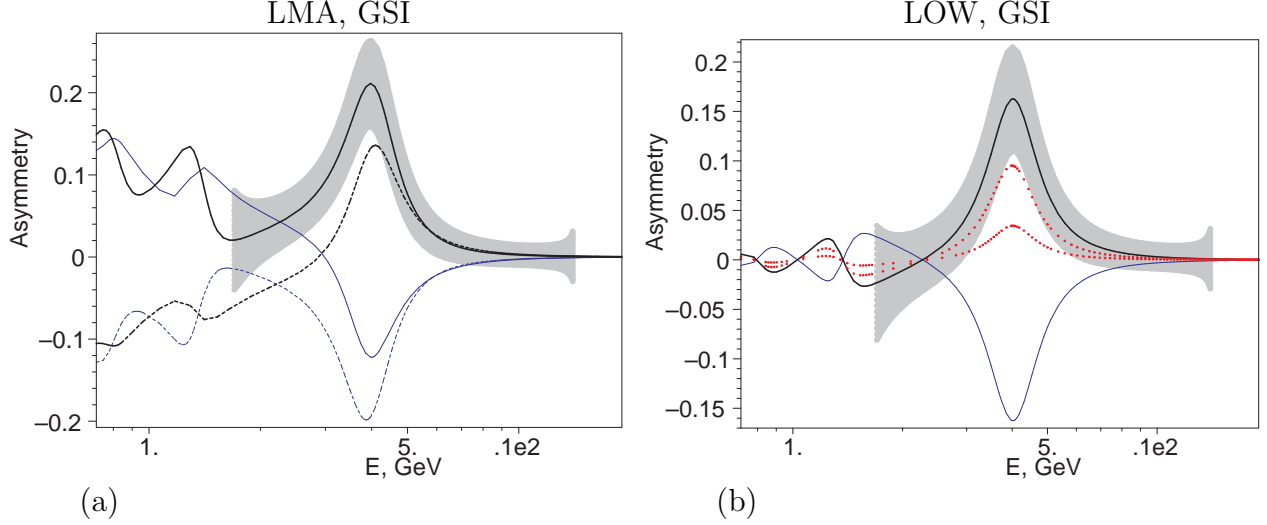


**Fig. 14.** Neutrino-antineutrino asymmetry as function of beam peak energy for the GSI ( $L = 2000$  km): (a) Point 1, (b) Point 2 (Eq. 3). Thick lines correspond to positive  $\Delta m_{32}^2$  while thin lines to negative ones. Solid lines are for  $\delta = 0^\circ$ , dashed lines are for  $\delta = 180^\circ$ . Wide grey strip shows errors in asymmetry with  $\delta = 0^\circ$  and  $\Delta m_{32}^2 > 0$ . Errors correspond to statistics for  $10^7$  s running time. Dotted lines in (b) are for  $s_{13}^2 = 0.01$  and  $0.03$  ( $\Delta m_{32}^2 > 0$ ); correspondence is as follows: the smaller the angle  $\theta_{13}$  the smaller the asymmetry.

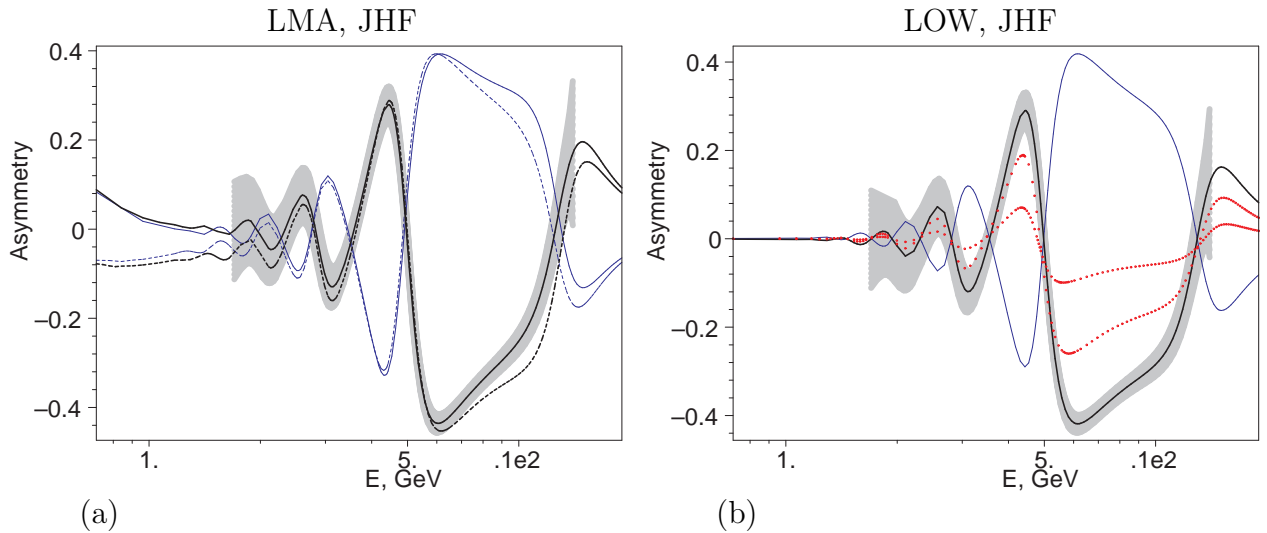


**Fig. 15.** The same as in Fig. 14, but for the JHF case ( $L = 7000$  km).

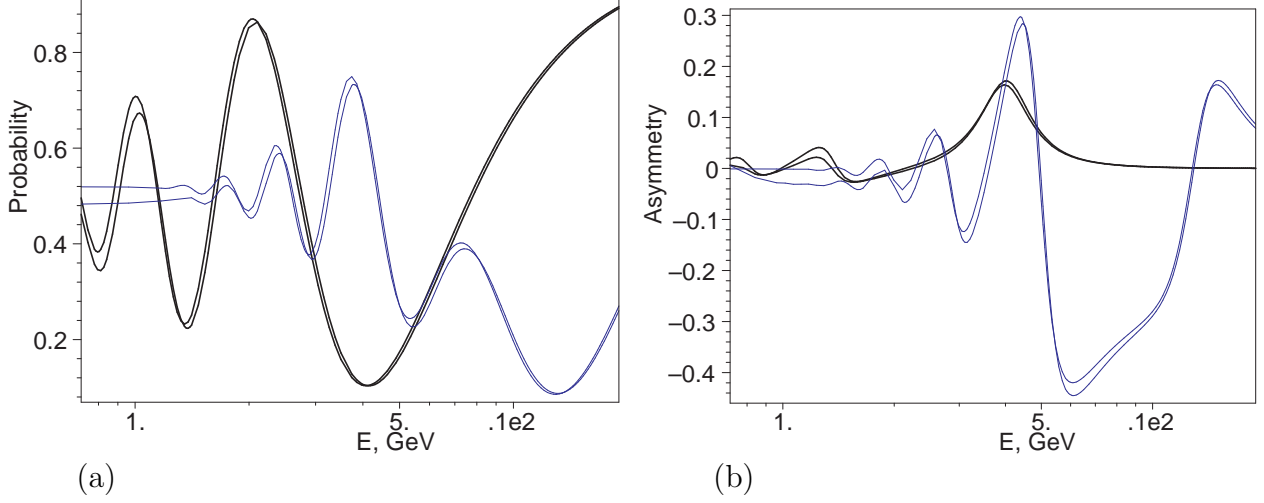


**Fig. 16.** Worse case to study: Point 1 and  $\delta = 90^\circ$  vs. Point 2 and any  $\delta$ . (a)  $P(\nu_\mu \rightarrow \nu_\mu)$ ; (b) Asymmetry. Two thick lines correspond to GSI ( $L = 2000$  km), Points 1 and 2, two thin lines correspond to JHF ( $L = 7000$  km), Points 1 and 2.

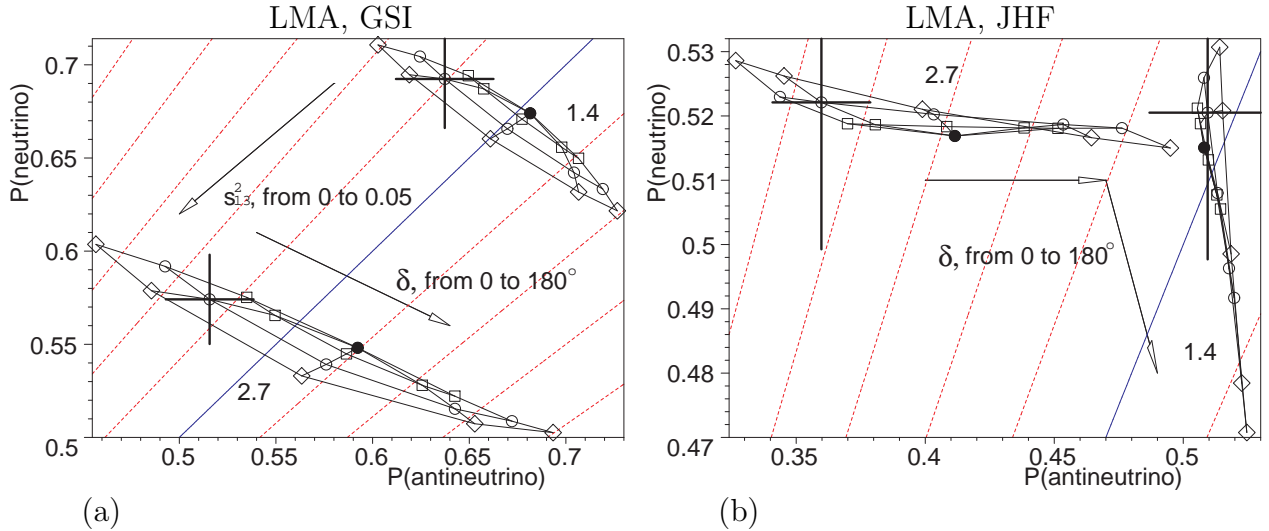


**Fig. 17.**  $P(\nu_\mu \rightarrow \nu_\mu)$  vs.  $P(\bar{\nu}_\mu \rightarrow \bar{\nu}_\mu)$  at  $E = 1$  GeV in dependence on phase  $\delta$  and  $s_{13}^2$  for Point 1: (a) for GSI, (b) for JHF. Regions for  $\Delta m_{21}^2 = 1.4 \cdot 10^{-4}$  eV<sup>2</sup> and  $\Delta m_{21}^2 = 2.7 \cdot 10^{-4}$  eV<sup>2</sup> are marked by “1.4” and “2.7”, respectively. One point corresponds to  $s_{13}^2 = 0$  (black circle) and five points with  $\delta = 0^\circ, 45^\circ, 90^\circ, 135^\circ$  and  $180^\circ$  (marked by the same symbols) are plotted for the values of  $s_{13}^2 = 0.01$  (boxes),  $0.03$  (circles) and  $0.05$  (diamonds). Straight line grid presents different values of asymmetry  $A_{CPT} = 0$  (solid line),  $\pm 0.04, \pm 0.08, \dots$  (dashed lines). The errors for point  $s_{13}^2 = 0.03$  and  $\delta = 45^\circ$ , which correspond to the statistics of  $10^3$  events in the absence of oscillations, are plotted.

The sensitivity to  $\delta$  depends on the value of  $s_{13}^2$  and the maximal sensitivity is for maximal allowed value of  $s_{13}^2 = 0.05$ . To comprehend the influence of  $s_{13}^2$  we calculated  $P(\nu_\mu \rightarrow \nu_\mu)$  and  $P(\bar{\nu}_\mu \rightarrow \bar{\nu}_\mu)$  at beam energy  $E = 1$  GeV for various values of  $s_{13}^2$  and  $\delta$ . Fig. 17 presents the results of these calculations. It contains two distinct regions which correspond to  $\Delta m_{21}^2 = 1.4 \cdot 10^{-4}$  eV<sup>2</sup> and  $\Delta m_{21}^2 = 2.7 \cdot 10^{-4}$  eV<sup>2</sup>. One can see that for the case of GSI there is one-to-one correspondence between points in the plane  $(P(\nu_\mu), P(\bar{\nu}_\mu))$  and values  $(s_{13}^2, \delta)$ . The typical errors, plotted for one point ( $s_{13}^2 = 0.03, \delta = 45^\circ$ ), allows to conclude that parameters  $s_{13}^2$  and  $\delta$  could be, in principle, disentangled and determined simultaneously. The situation for the case of JHF is more involved. The one-to-one correspondence is lost and the relative variations in oscillation probabilities with  $s_{13}^2$  and  $\delta$  are smaller than in the GSI case. Qualitatively this can be understood as the increasing role of matter effects. The last ones become dominant even at relatively low energies, where the sensitivity to  $\delta$  is maximal.

Considered in this section topics allow to make a comparison between GSI and JHF as the sites for neutrino beam source. If LMA solution is realized in Nature, GSI can provide more information on oscillation parameters in the low energy measurements. JHF is more sensitive to the parameters of LOW region at higher energies where the matter effects maximize asymmetry  $A_{CPT}$ .

## 5 Conclusion

The VLBL neutrino oscillation experiment (baseline of 2000–7000 km) with the UNK  $\sim 1$  Mton underground detector will provide:

- Observation of the oscillation patterns for the  $\nu_\mu$  and  $\bar{\nu}_\mu$  disappearance in the  $0.5 \cdot 10^{-3} < \Delta m^2 < 6 \cdot 10^{-3}$  eV<sup>2</sup> range using the NB neutrino beam.
- Direct observation of the matter effects by comparison of  $\nu_\mu$  and  $\bar{\nu}_\mu$  oscillation curves.

It allows to extract important physical information such as

1. Measurement of the  $\Delta m_{32}^2$  and the intensity of oscillations with the accuracy at the level of  $\sim 1\%$ .
2. Measurement of  $\sin^2 \theta_{13}$  down to the value of  $\sim 0.01$ .
3. Unambiguous determination of the sign of  $\Delta m_{32}^2$  by the sign of asymmetry  $A_{CPT}$  for  $\sin^2 \theta_{13} \gtrsim 0.01$ .
4. Distinction between LMA and LOW solutions outside the case of some exceptional values of mixing matrix parameters.
5. Determination of  $CP$  violating phase  $\delta$  in the case of LMA solution.

Thus, the experiment allows to prove the standard scenario of neutrino oscillations, to measure precisely essential oscillation parameters as well as to search for new phenomena.

## Acknowledgements

The authors are thankful to A. Logunov, A. Miagkov, R. Nahnauer, V. Ryabov, V. Tsarev and N. Tyurin for useful discussions. One of us (VA) is very grateful to the Organizers of the 1-st International Workshop on Nuclear and Particle Physics at 50-GeV PS (KEK, Tsukuba, Japan, Dec.10–12, 2001) for giving him opportunity to present the talk on this matter at the Workshop.

## References

- [1] Y. Fukuda et al., Phys. Lett. B433 (1998), 9;  
Y. Fukuda et al., Phys. Lett. B436 (1998), 3;  
Y. Fukuda et al., Phys. Rev. Lett. B81 (1998), 1562.
- [2] M. Ambrosio et al., Phys. Lett. B434 (1998), 451.
- [3] P. S. Vasiliev et al., *On the possibility to study neutrino oscillations at Gran-Sasso (Italy) detectors with the use of beams from the 600 GeV UNK accelerator*, Proc. of Workshop “UNK-600”, Protvino, 1994, p. 165 (in Russian).
- [4] C. Yanagisawa, Nucl. Phys. Proc. Suppl. 95 (2001), 130.
- [5] P. Adamson et al., *The MINOS detector technical design report*, Fermilab Report NUMI-L-337, October 1998.
- [6] G. Acquistapace et al. *The CERN Neutrino Beam to Gran Sasso*, Report CERN 98-02 and INFN/AE-98/05;  
R.Bailey et al., Addendum, CERN Report-SL/99-034(DI) and INFN/AE-99/05.
- [7] Y. Itow et al., *The JHF-Kamioka neutrino project*, KEK report 2001-4, ICRR-report-477-2001-7, TRI-PP-01-05, hep-ex/0106019.
- [8] M. Aoki et al. *Prospects of Very Long Base-Line Neutrino Oscillation Experiments with the KEK-JAERI High Intensity Proton Accelerator*, KEK-TH-798, VPI-IPPAP-01-03, hep-ph/0112338;  
Hesheng Chen et al., *Prospect of a very long baseline neutrino oscillation experiment: HIPA to Beijing*, IHEP-EP-2001-01, AS-ITP-2001-004, AMES-HEP-01-01, hep-ph/0104266.
- [9] A. Blondel et al., Nucl. Instr. and Meth. A451 (2000), 102.
- [10] T.Toshito (SuperKamiokande Collaboration), *SuperKamiokande atmospheric neutrino results*, hep-ex/0105023.
- [11] M. Apollonio et al., Phys. Lett. B466 (1999), 415.
- [12] V. Barger, J. G. Learned, S. Pakvasa and T. J. Weiler, Phys. Rev. Lett. 82 (1999), 2640.
- [13] A. Gago et al, *Testing flavor changing neutrino interactions in long baseline experiments*, hep-ph/9911470.

- [14] G. Dvali and A. Smirnov, Nucl. Phys. B563 (1999), 63.
- [15] Zhi-zhong Xing, J. Phys. G28 (2002), B7, hep-ph/0112120.
- [16] G. Barenboim et al., *Neutrinos as the Messengers of CPT violation*, Preprint FERMILAB-PUB-01-235-T, hep-ph/0108199.
- [17] A. Leick, *Global Positioning System Satellite Surveying*, 2-nd edition, Wiley-Interscience, 1995.
- [18] A. G. Abramov et al., *Beam Optics and Target Conceptual Designs for the NuMI Project*, Preprint IHEP 2001-2, Protvino, 2001.
- [19] S. Belikov et al., *Physical characteristics of the PMMA shifter SOFZ-105*, Preprint IHEP 92-55, Protvino, 1992 (in Russian).
- [20] V. Abramov et al., Nucl. Instr. and Meth. A419 (1998), 660.
- [21] S. Belikov et al., *The performance of FEU-115M Photomultiplier Tubes for the PHENIX Electromagnetic Calorimeter*, Instruments and Experimental Techniques, Vol.40, No.3 1997, p. 333; Preprint IHEP 96-42, Protvino, 1996 (in Russian).
- [22] M. Ambrosio et al., MACRO Collaboration, Astropart. Phys. 9 (1998), 105, hep-ex/9807032.
- [23] For recent review and extensive references, see M. C. Gonzalez-Garcia and Y. Nir, *Developments in neutrino physics*, Preprint CERN-TH-2002-021, hep-ph/0202058.
- [24] A. M. Dziewonski and D. L. Anderson, *Preliminary Reference Earth Model*, Phys. Earth Planet. Inter., Vol. 25, 1981, p. 297.